LUND UNIVERSITY

Iterative Reference Learning for Cartesian Impedance Control of Robot Manipulators

Salt Ducaju, Julian; Olofsson, Björn; Johansson, Rolf

LUND UNIVERSITY

PO Box 117
221 00 Lund
+46 46-222 00 00

Iterative Reference Learning for Cartesian Impedance Control of Robot Manipulators

Julian M. Salt Ducaju, Björn Olofsson, Rolf Johansson

Abstract— In this paper, an iterative learning strategy was developed to improve trajectory tracking for an impedance-controlled robot manipulator. In this learning strategy, an update law was proposed to modify the Cartesian reference of an impedance controller. Also, the conditions that ensure its convergence considering the dynamics of the robot were derived. Finally, an experimental evaluation was performed using a Franka Emika Panda robot in two different robot tasks, and its results showed that robot task completion was achieved in a lower number of iterations, while maintaining a smooth physical interaction between the robot and its surroundings.

I. INTRODUCTION

Recent trends in manufacturing industry to replace mass production for mass customization could not be adequately addressed in industrial settings characterized by a fixed-structure workplace [1]. To avoid these limitations in modern-day industrial environments, manufacturing processes should be able to adapt with ease to rapidly changing requirements. Kinesthetic teaching has been proposed for this purpose in the last years, since it is a human–robot collaboration strategy where a human collaborator manually guides a robot to define or modify a robot trajectory [2], thus allowing the use of human dexterity and intelligence in robot task adaptation [3].

In less structured industrial environments, indirect force-control strategies, such as impedance control [4], [5], are widely used, since, compared to other force-control strategies, they rely less on an accurate description of the robot environment [6]. Impedance control regulates the interacting forces between a robot and its environment by modeling the external force applied to the robot as a mass-spring-damper relationship to handle the mismatch between the robot state and a user-defined reference. By regulating the interaction force between a robot and its environment, impedance control allows physical guidance of a robot by human operators, and provides physical safety to the actors involved. However, the dynamical relationship imposed by impedance-control strategies inherently introduces a deviation in the robot trajectory which might cause a robot not to complete its designated task, *e.g.*, an insertion task where the peg–hole tolerance is small.

Several strategies proposed in the past to improve trajectory tracking in a robotic manipulator might cause undesired effects in collaborative environments. First, position-feedback control [7] would modify the interaction forces between the robot and its environment by increasing the robot stiffness, which might damage the manipulated objects and pose a safety threat to robots and/or humans involved. Also, other strategies that consist in trajectory scaling [8], [9] would inherently slow down the execution of the robot motion with task completion at stake if the dynamics of the robot are not fully modeled, *e.g.*, joint elasticity or friction.

Moreover, strategies based on learning the desired robot behavior could be used in this context. Among these strategies, Reinforcement Learning (RL) has gained popularity in recent years [10], although it might still be too time-consuming for these robot applications, since this strategy often requires a high number of trials to learn a desired robot behavior [11]. Also, Iterative Learning Control (ILC) [12], [13] has been used extensively in the past to improve robot behavior. Nevertheless, in its linear formulation [14], [15], ILC might not fully allow to exploit the robot dynamics. Alternatively, model-based adaptive control [16] or adaptive iterative learning techniques (AILC) [17], [18] can deal with robot nonlinearities, while relieving the high-stiffness requirements of previously-proposed strategies [19] (which had the same limitations as position-feedback controllers [7] for physical interaction). However, the adaptive terms in AILC would result in real-time modifications of the impedance behavior of a robot [20]. Finally, the use of learning techniques for impedance-controlled robots has been explored in the past [21], [22], but it was focused on impedance matching, *i.e.*, matching a desired physical interaction, instead of reducing trajectory tracking error.

In this paper, we address the problem of improving trajectory tracking in robotic applications where impedance control is used by proposing an iterative learning strategy, namely, Iterative Reference Learning Controller (IRLC), that provides a Cartesian reference update. To validate our proposal, several experiments have been performed using a real robotic manipulator: a peg-in-hole experiment and a snap-fit assembly of a switch.

The paper is organized as follows: Sec. II introduces the dynamics model used for Cartesian impedance control of robot manipulators. Then, Sec. III presents an iterative reference learning strategy to improve trajectory tracking, which was extensively evaluated with a real robot in experiments presented in Sec. IV. Finally, a discussion is included in Sec. V and conclusions are drawn in Sec. VI.

II. Modeling Background

The dynamic behavior of a robot manipulator controlled by a Cartesian impedance strategy is introduced in this section.

A. Robot Dynamics

The dynamics of the robot can be written in the joint space of the robot, $q \in \mathbb{R}^n$, as [23]

$$M(q)\ddot{q} + C(q,\dot{q})\dot{q} + G(q) = \tau + \tau^{\text{ext}} \tag{1}$$

where $M(q) \in \mathbb{R}^{n \times n}$ is the generalized inertia matrix (which is symmetric positive definite), $C(q,\dot{q}) \in \mathbb{R}^{n \times n}$ describes the Coriolis and centripetal forces effects, and $G(q) \in \mathbb{R}^n$ captures the gravity-induced torques. Finally, $\tau \in \mathbb{R}^n$ represents the input torques, n being the number of joints of the robot, and $\tau^{\text{ext}} \in \mathbb{R}^n$ are the external torques.

Moreover, the rigid-body equation of the robot can be rewritten in terms of its end-effector pose $\xi \in \mathbb{R}^m$, which is composed by the position and orientation of the end-effector (often, $m = 6$)

$$M_\xi(q)\ddot{\xi} + C_\xi(q,\dot{q})\dot{\xi} + G_\xi(q) = F + F^{\text{ext}} \tag{2}$$

where $F \in \mathbb{R}^m$ is the input force, and $F^{\text{ext}} \in \mathbb{R}^m$ the external Cartesian forces. Additionally, for a fully-actuated nonredundant robot ($n = m$), $M_\xi \in \mathbb{R}^{m \times m}$, $C_\xi \in \mathbb{R}^{m \times m}$, and $G_\xi \in \mathbb{R}^m$ are equal to

$$M_\xi = J^{-\text{T}}(q)M(q)J^{-1}(q) \tag{3}$$
$$C_\xi = J^{-\text{T}}(q)(C(q,\dot{q}) - M(q)J^{-1}(q)\dot{J}(q))J^{-1}(q) \tag{4}$$
$$G_\xi = J^{-\text{T}}(q)G(q) \tag{5}$$

assuming that the Jacobian relative to the base frame of the robot, $J(q) \in \mathbb{R}^{m \times m}$, has full rank [24].

Furthermore, it is relevant to highlight two properties of a robot manipulator [25]:

- The robot inertia matrix M_ξ in Eq. (2) is a positive definite matrix,

$$x^{\text{T}} M_\xi x > 0, \quad \forall x \neq 0 \tag{6}$$

- The matrix $\dot{M}_\xi - 2C_\xi$ is skew symmetric,

$$x^{\text{T}}\left(\dot{M}_\xi - 2C_\xi\right)x = 0, \quad \forall x \neq 0 \tag{7}$$

B. Robot Cartesian Impedance Control

An input force F in Eq. (2) equal to

$$F = K\Delta\xi - D\dot{\xi} + G_\xi(q) \tag{8}$$

would achieve a Cartesian impedance control of the robot end-effector [4], *i.e.*, a mass-spring-damper relationship between the Cartesian pose offset from its reference, $\Delta\xi = \xi_d - \xi$ (ξ_d being the Cartesian reference) and the external Cartesian force F^{ext},

$$F^{\text{ext}} = M_\xi(q)\ddot{\xi} + (C_\xi(q,\dot{q}) + D)\dot{\xi} - K\Delta\xi \tag{9}$$

where $K \in S_{++}^m$ and $D \in S_{++}^m$ (S_{++} denoting symmetric positive-definiteness) are diagonal matrices that represent the control-induced stiffness and damping, respectively.

III. Iterative Reference Learning Control

An iterative learning strategy to improve the Cartesian trajectory tracking for a Cartesian impedance-controlled robot is presented in this section.

A. Robot Input Feedforward and Error Dynamics

The input force F in Eq. (2) commanded to the robot could include an additional feedforward term F_{ff} [17], [19] computed using iterative learning

$$F = F_{fb} + F_{ff} \tag{10}$$

where $F_{ff} = 0$ at the first learning iteration, and the input force feedback term F_{fb} is given by the desired Cartesian impedance behavior in Eq. (9). Then, choosing an error variable $e(t) \in \mathbb{R}^6$ with respect to a desired Cartesian pose, $\xi_R \in \mathbb{R}^6$, as

$$e = \xi_R - \xi \tag{11}$$

the error dynamics of the system in the absence of external forces acting on the robot would be equal to

$$M_\xi\ddot{e} + (C_\xi + D)\dot{e} + Ke = -F_{ff} \tag{12}$$

with $\dot{\xi}_R = \ddot{\xi}_R = 0$.

B. Learning Update Law

The force input feedforward strategy, F_{ff} in Eq. (10), at iteration $i + 1$ could be chosen as:

$$^{i+1}F_{ff} = {}^{i}F_{ff} + \beta D\,{}^{i}\zeta \tag{13}$$

where $\beta > 0$ is the iterative learning gain and $^i\zeta \in \mathbb{R}^6$ is formulated considering the pose error e and its time derivative $\dot{e}$, similar to [17], [19],

$$^i\zeta = {}^i\dot{e} + R\,{}^i e \tag{14}$$

with $R \in \mathbb{R}^{6 \times 6}$ being a diagonal matrix

$$R = D^{-1}(K - \Upsilon) > 0 \tag{15}$$

and $\Upsilon \in \mathbb{R}^{6 \times 6}$ also being diagonal.

Then, considering Eqs. (8), (10), and (13), the update law at iteration $i + 1$ for the Cartesian impedance controller reference used in Eq. (9) would be

$$^{i+1}\xi_d = {}^i\xi_d + \beta K^{-1}D\left[R(\xi_R - {}^i\xi) - {}^i\dot{\xi}\right] \tag{16}$$

where $^0\xi_d = \xi_R$.

Remark. *The impedance-controlled robot behavior resulting from an iterative strategy where ξ_d in Eq. (9) is modified at every iteration step so that the error signal e in Eq. (11) converges to 0, would be stable by design; see [26, Lemma III.2] for more details of the stability justification.*

The structure for the proposed Iterative Reference Learning Controller (IRLC) is illustrated in Fig. 1. It can be seen that at every iteration, the Cartesian impedance reference sent to the controller is calculated considering the robot motion at the previous iteration, and the desired Cartesian pose.
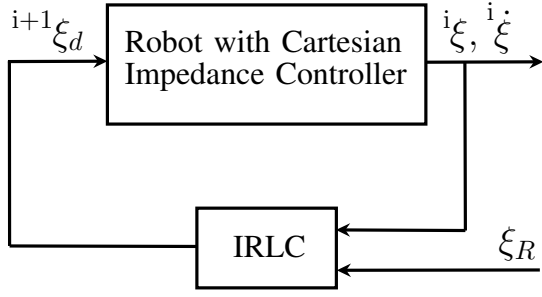
Fig. 1. Illustration of the iterative learning controller proposed to reduce the robot trajectory error.

Moreover, after $N > 0$ iterations, the update law in Eq. (16) is equivalent to:

$$^{N}\xi_d = \xi_R + \beta K^{-1} D \Big[R \Big(N\xi_R - \sum_{j=0}^{N-1} {}^{j}\xi \Big) - \sum_{j=0}^{N-1} {}^{j}\dot{\xi} \Big] \quad (17)$$

C. Convergence Analysis

A convergence analysis of the update law provided in Sec. III-B is presented in this section. Convergence has been shown by proving the monotonous decrease of a performance index, as established in [19]. The differences between the performance index in [19] and our proposal are highlighted in Sec. V.

Theorem III.1. *The proposed update law in Eq. (16) would allow ξ to converge to ξ_R provided that the learning gain $\beta > 0$ of the iterative scheme is chosen so that the following conditions are fulfilled:*

$$g_{\dot{e}} \triangleq (2 - \beta)\lambda_{\mathrm{m}}(D) - 2R\lambda_{\mathrm{M}}(M_\xi) > 0 \quad (18)$$

$$g_e \triangleq (2 - \beta)\lambda_{\mathrm{m}}(D) - 2\lambda_{\mathrm{M}}(C_\xi)$$
$$+ 2\lambda_{\mathrm{m}}(R^{-1}\Upsilon) > 0 \quad (19)$$

$$\sqrt{g_{\dot{e}} g_e} > \lambda_{\mathrm{M}}(R^{-1}\Upsilon - RM_\xi - C_\xi) \quad (20)$$

where λ_{m} and λ_{M} refer to the minimum and maximum eigenvalues, for all $t \in [0, t_{\mathrm{F}}]$, respectively, with t_{F} being the final time of the robot task execution.

Proof: The monotonous decrease of performance index

$$^{i}V = \beta \int_0^t \big({}^{i}\zeta\big)^{\mathrm{T}} D\big({}^{i}\zeta\big) dt > 0 \quad (21)$$

at each iteration step i can be shown. First, using this performance index and Eq. (13),

$$^{i+1}V = \beta \int_0^t \big({}^{i+1}\zeta\big)^{\mathrm{T}} D\big({}^{i+1}\zeta\big) dt =$$
$$= \beta \int_0^t \big({}^{i}\zeta\big)^{\mathrm{T}} D\big({}^{i}\zeta\big) dt$$
$$+ \beta \int_0^t \Big[\big({}^{i}\Delta\zeta\big)^{\mathrm{T}} D\big({}^{i}\Delta\zeta\big) + 2\big({}^{i}\Delta\zeta\big)^{\mathrm{T}} D\,{}^{i}\zeta\Big] dt \quad (22)$$

where ${}^{i+1}\zeta = {}^{i}\zeta + {}^{i}\Delta\zeta$. Then, the error dynamics of the system in Eq. (12) expressed in terms of the variable $\Delta\zeta$

(and assuming that M_ξ and C_ξ do not vary between the same sample time of consecutive iterations) is equal to

$$M_\xi\,{}^{i}\Delta\dot{\zeta} + (C_\xi + D - RM_\xi)\,{}^{i}\Delta\zeta +$$
$$(-RC_\xi + R^2 M_\xi + \Upsilon)\,{}^{i}\Delta e = -\beta D\,{}^{i}\zeta \quad (23)$$

since

$$^{i}\Delta\zeta = {}^{i}\Delta\dot{e} + R\,{}^{i}\Delta e \quad (24)$$

$$^{i}\Delta F_{ff} = \beta D\,{}^{i}\Delta\zeta \quad (25)$$

and it can be obtained that

$$^{i}\Delta V = {}^{i+1}V - {}^{i}V = \int_0^t \Big[\beta \big({}^{i}\Delta\zeta\big)^{\mathrm{T}} D\big({}^{i}\Delta\zeta\big)$$
$$- 2\big({}^{i}\Delta\zeta\big)^{\mathrm{T}} M_\xi\,{}^{i}\Delta\dot{\zeta}$$
$$- 2\big({}^{i}\Delta\zeta\big)^{\mathrm{T}} (C_\xi - D - RM_\xi)\,{}^{i}\Delta\zeta$$
$$- 2\big({}^{i}\Delta\zeta\big)^{\mathrm{T}} (R^2 M_\xi - RC_\xi + \Upsilon)\,{}^{i}\Delta e \Big] dt \quad (26)$$

Moreover,

$$\frac{d}{dt}\Big(\big({}^{i}\Delta\zeta\big)^{\mathrm{T}} M_\xi\,{}^{i}\Delta\zeta\Big) = \big({}^{i}\Delta\zeta\big)^{\mathrm{T}} \dot{M}_\xi\,{}^{i}\Delta\zeta + 2\big({}^{i}\Delta\zeta\big)^{\mathrm{T}} M_\xi\,{}^{i}\Delta\dot{\zeta} \quad (27)$$

so Eq. (26) can be rewritten as

$$^{i}\Delta V = -\big({}^{i}\Delta\zeta\big)^{\mathrm{T}} M_\xi\big({}^{i}\Delta\zeta\big) + \int_0^t \Big[\big({}^{i}\Delta\zeta\big)^{\mathrm{T}} \dot{M}_\xi\big({}^{i}\Delta\zeta\big)$$
$$+ \beta \big({}^{i}\Delta\zeta\big)^{\mathrm{T}} D\big({}^{i}\Delta\zeta\big)$$
$$- 2\big({}^{i}\Delta\zeta\big)^{\mathrm{T}} (C_\xi + D - RM_\xi)\big({}^{i}\Delta\zeta\big)$$
$$- 2\big({}^{i}\Delta\zeta\big)^{\mathrm{T}} (R^2 M_\xi - RC_\xi + \Upsilon)\big({}^{i}\Delta e\big) \Big] dt \quad (28)$$

Since M_ξ is positive definite, Eq. (6), and $\dot{M}_\xi - 2C_\xi$ is a skew-symmetric matrix, Eq. (7),

$$^{i}\Delta V \leq \int_0^t \Big[\beta \big({}^{i}\Delta\zeta\big)^{\mathrm{T}} D\big({}^{i}\Delta\zeta\big)$$
$$- 2\big({}^{i}\Delta\zeta\big)^{\mathrm{T}} (D - RM_\xi)\big({}^{i}\Delta\zeta\big)$$
$$- 2\big({}^{i}\Delta\zeta\big)^{\mathrm{T}} (R^2 M_\xi - RC_\xi + \Upsilon)\big({}^{i}\Delta e\big) \Big] dt \quad (29)$$

which is equivalent to

$$^{i}\Delta V \leq \int_0^t \Big[\big({}^{i}\Delta\zeta\big)^{\mathrm{T}} ((\beta - 2)D + 2RM_\xi)\big({}^{i}\Delta\zeta\big)$$
$$- 2\big({}^{i}\Delta\zeta\big)^{\mathrm{T}} (R^2 M_\xi - RC_\xi + \Upsilon)\big({}^{i}\Delta e\big) \Big] dt \quad (30)$$

Using Eq. (14) to substitute ${}^{i}\Delta\zeta$,

$$\int_0^t \big({}^{i}\Delta\zeta\big)^{\mathrm{T}} ((\beta - 2)D + 2RM_\xi)\big({}^{i}\Delta\zeta\big) dt =$$
$$\int_0^t \big({}^{i}\Delta\dot{e}\big)^{\mathrm{T}} ((\beta - 2)D + 2RM_\xi)\big({}^{i}\Delta\dot{e}\big) dt$$
$$+ \int_0^t \big(R\,{}^{i}\Delta e\big)^{\mathrm{T}} ((\beta - 2)D + 2RM_\xi)\big(R\,{}^{i}\Delta e\big) dt$$
$$+ 2\int_0^t \big(R\,{}^{i}\Delta e\big)^{\mathrm{T}} ((\beta - 2)D + 2RM_\xi)\big({}^{i}\Delta\dot{e}\big) dt \quad (31)$$

and

$$\int_0^t -2\left(^{\mathrm{i}}\Delta\zeta\right)^{\mathrm{T}}(R^2 M_\xi - RC_\xi + \Upsilon)\left(^{\mathrm{i}}\Delta e\right)dt =$$
$$-2R\int_0^t \left(^{\mathrm{i}}\Delta e\right)^{\mathrm{T}}(RM_\xi - C_\xi + R^{-1}\Upsilon)\left(R\,^{\mathrm{i}}\Delta e\right)dt$$
$$-2\int_0^t \left(^{\mathrm{i}}\Delta\dot{e}\right)^{\mathrm{T}}(RM_\xi - C_\xi + R^{-1}\Upsilon)\left(R\,^{\mathrm{i}}\Delta e\right)dt \quad (32)$$

Therefore,

$$^{\mathrm{i}}\Delta V \leq \int_0^t \left(^{\mathrm{i}}\Delta\dot{e}\right)^{\mathrm{T}}((\beta-2)D + 2RM_\xi)\left(^{\mathrm{i}}\Delta\dot{e}\right)dt$$
$$+2\int_0^t \left(^{\mathrm{i}}\Delta\dot{e}\right)^{\mathrm{T}}((\beta-2)D + RM_\xi + C_\xi$$
$$-R^{-1}\Upsilon)\left(R\,^{\mathrm{i}}\Delta e\right)dt + \int_0^t \left(R\,^{\mathrm{i}}\Delta e\right)^{\mathrm{T}}((\beta-2)D$$
$$+2C_\xi - 2R^{-1}\Upsilon)\left(R\,^{\mathrm{i}}\Delta e\right)dt \quad (33)$$

Then, applying integration by parts,

$$^{\mathrm{i}}\Delta V \leq \int_0^t \left(^{\mathrm{i}}\Delta\dot{e}\right)^{\mathrm{T}}((\beta-2)D + 2RM_\xi)\left(^{\mathrm{i}}\Delta\dot{e}\right)dt$$
$$+2\int_0^t \left(^{\mathrm{i}}\Delta\dot{e}\right)^{\mathrm{T}}(RM_\xi + C_\xi - R^{-1}\Upsilon)\left(R\,^{\mathrm{i}}\Delta e\right)dt$$
$$+\int_0^t \left(R\,^{\mathrm{i}}\Delta e\right)^{\mathrm{T}}((\beta-2) - 2R^{-1}\Upsilon + 2C_\xi)\left(R\,^{\mathrm{i}}\Delta e\right)dt$$
$$+\left(^{\mathrm{i}}\Delta e\right)^{\mathrm{T}}D((\beta-2)D)\left(R\,^{\mathrm{i}}\Delta e\right) \quad (34)$$

where $\left(^{\mathrm{i}}\Delta e\right)^{\mathrm{T}}((\beta-2)D)\left(R\,^{\mathrm{i}}\Delta e\right) \leq 0$ for $\beta < 2$. This expression can be rewritten as

$$^{\mathrm{i}}\Delta V \leq -\int_0^t \begin{bmatrix} ^{\mathrm{i}}\Delta\dot{e} \\ R\,^{\mathrm{i}}\Delta e \end{bmatrix}^{\mathrm{T}} \Omega \begin{bmatrix} ^{\mathrm{i}}\Delta\dot{e} \\ R\,^{\mathrm{i}}\Delta e \end{bmatrix} dt \quad (35)$$

for

$$\Omega = \begin{bmatrix} g_{\dot{e}}I_6 & R^{-1}\Upsilon - RM_\xi - C_\xi \\ R^{-1}\Upsilon - RM_\xi - C_\xi & g_e I_6 \end{bmatrix} \quad (36)$$

where $I_6 \in \mathbb{R}^{6\times6}$ represents an identity matrix. If conditions (18), (19), (20) are fulfilled, $\Omega \geq 0$, *i.e.*, all the eigenvalues of Ω would be nonnegative. Therefore, $^{\mathrm{i}}\Delta V \leq 0$, where $^{\mathrm{i}}\Delta V = 0$ would only hold for $^{\mathrm{i}}\Delta e = ^{\mathrm{i}}\Delta\dot{e} = 0$.

As discussed in [19], where a performance index similar to the one in Eq. (21) was used, this would imply that $\lim_{\mathrm{i}\to\infty}{}^{\mathrm{i}}e(t) = 0$ for all $t \in [0, t_\mathrm{F}]$, assuming that $^{\mathrm{i}}\dot{e}(0) = ^{\mathrm{i}}e(0) = 0$ for all i. ∎

IV. EXPERIMENTS

The IRLC strategy proposed in Sec. III was evaluated for several robot tasks.

A. Application Scenario

As introduced in Sec. I, kinesthetic teaching [27] allows a human operator to manually guide a robot manipulator to define or to correct a robot trajectory, which corresponds to a certain robot task (Fig. 2). However, a robot controlled with an impedance controller, such as the Cartesian impedance controller in Eq. (8) that uses these operator-defined Cartesian poses as references might not be able to complete its task because of the trajectory-tracking deviation introduced by these controllers (to the advantage of allowing physical interaction between the robot and its surroundings).

Therefore, the goal of the experiments presented in this section is to evaluate if the iterative learning strategy proposed in Sec. III would allow a robot to complete its desired task by updating a manually-defined Cartesian reference used in a Cartesian impedance-controlled robot.

The experiments presented in this section were performed using a Franka Emika Panda [28] robot mounted on a table, as shown in Fig. 2. Since robot joint redundancy is out of the scope of this paper, the seventh joint of the robot was locked at $\theta_7 = \pi/2$ rad, and only the first six joints of the robot were controlled. The robot was controlled at a sampling rate equal to 1 kHz.

Fig. 2. A human operator manually guiding a Franka Emika Panda [28] robot mounted on a table to define the desired robot Cartesian poses, ξ_R in Eq. (11), for a peg-in-hole task.

B. Peg-in-Hole Task

In a peg-in-hole robot task, a robot manipulator should insert a peg (in this experiment, with cylindrical shape) attached to its end-effector in a hole whose dimensions are slightly larger than the ones of the peg.

For this experiment, the Cartesian impedance values selected were:

- The virtual stiffness K was chosen as 150 [N/m] for the translational degrees of freedom and as 15 [N/rad] for the rotational degrees of freedom.
- The virtual damping D was chosen as 50 [Ns/m] for the translational degrees of freedom and as 10 [Ns/rad] for the rotational degrees of freedom.

Moreover, for the learning update law (presented in Sec. III-B), the Cartesian impedance parameters selected (K and D), together with the iterative convergence conditions (18)–(20) of Theorem III.1, allowed to choose $\beta = 0.5$, and $R = 2.5$ for the translational degrees of freedom and $R = 0.92$ for the rotational degrees of freedom.

The results for this experiment are shown in Figs. 3, 4, and 5. Figure 3 shows the temporal evolution of the end-effector position of the robot. It can be seen in Fig. 3 that before using the iterative learning strategy proposed (*No IRLC*), the Cartesian impedance controller deviated from the desired trajectory (ξ_R), which prevented the robot to complete its task, *i.e.*, to insert the peg in the hole. This is also shown in the left image of Fig. 4, which displays the position of the peg once the robot trajectory is executed for two different scenarios: before learning (left) and after learning (right). Finally, Fig. 3 shows that the deviation with respect to the desired trajectory decreased at every learning iteration, with the robot being able to complete its task after only two learning iterations. Consistent with the tracking-error reduction at each learning iteration, the performance index $^i V$ of Eq. (21) decreased at each iteration, *i.e.*, the performance index increment, $^i \Delta V$ of Eq. (26), is negative for all learning iterations, as shown in Fig. 5, which matches the convergence analysis of this method presented in Theorem III.1.
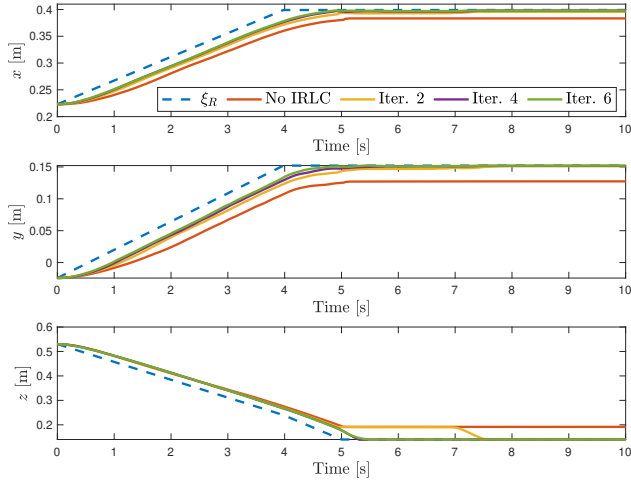

Fig. 3. Temporal evolution of the position of the robot end-effector along each Cartesian direction x, y, z with respect to its desired values for a peg-in-hole task.
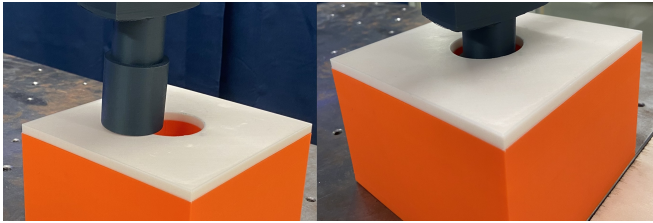

Fig. 4. Comparison between the final position of the peg before the proposed iterative learning strategy was used (left) and after six iterations of the proposed learning controller (right) for a peg-in-hole task.

1) Comparison with an Alternative ILC Method: The benefits of the iterative reference learning proposal presented in Sec. III is highlighted by comparing its performance to one of the methods that have been used extensively in literature, *e.g.*, [29], [30] for recent examples, namely ILC
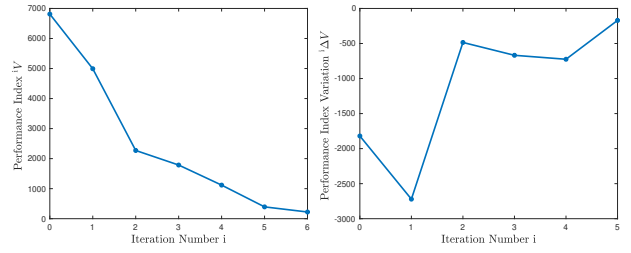

Fig. 5. Performance index (left), $^i V$ of Eq. (21), and performance index increment (right), $^i \Delta V$ of Eq. (26), for each learning iteration i for a peg-in-hole task.

[14]. An ILC strategy could be defined using an input update law

$$^{i+1}U(z) = Q(z)(^i U(z) + L(z)\,^i E(z)) \qquad (37)$$

with $^i E(z) = Y_R(z) -\,^i Y(z)$ being the output error signal, $L(z)$ representing a learning filter, $Q(z)$ being a low-pass filter used to improve the robustness of the ILC method, and z representing the discrete-time operator. Then, m transfer functions were obtained from the Cartesian impedance behavior of the robot in Eq. (9) during the initial execution of the peg-insertion task. Each output, $y_m \in \mathbb{R}$, of the system would be equal to the corresponding component of ξ and each input, $u_m \in \mathbb{R}$, of the system would be equal to the corresponding component of ξ_R. The transfer functions obtained, in the Laplace domain, are

$$G_c(s) = \frac{\omega_n^2}{s^2 + 2\delta\omega_n s + \omega_n^2} \qquad (38)$$

with $\omega_n = 3.78$ rad/s and $\delta = 0.64$ for the position DOFs, and $\omega_n = 2.58$ rad/s and $\delta = 1.44$ for the orientation DOFs, which are then discretized using a zero-order-hold (ZOH) method at the sample period of the robot, *i.e.*, $h = 0.001$ s, to obtain each $G(z)$. The learning gain $L(z)$ in Eq. (37) was chosen as

$$L(z) = \widetilde{G}^{-1}(z)(1 - H(z)) \qquad (39)$$

with $\widetilde{G}^{-1}(z)$ being an approximation to the inverse of $G(z)$, where the inverted zeros of $G(z)$ that were close to the unit circle were replaced with static gains to avoid obtaining a ringing behavior [15], and $H(z)$ is a first-order high-pass filter used to determine the convergence rate [14]. The selection of the learning gain $L(z)$ as in Eq. (39) together with choosing $Q(z)$ as a first-order low-pass filter with cut-off frequency $\omega_c = 50$ Hz fulfills the convergence criteria for this formulation [14]

$$\sup_{\omega \in [-\pi, \pi]} \left|\left| 1 - G(e^{i\omega h})L(e^{i\omega h}) \right|\right| < Q(e^{i\omega h})^{-1} \qquad (40)$$

for all DOFs.

Figures 6 and 7 show a comparison between the proposed IRLC solution presented in Sec. III and the alternative ILC method. The differences in the temporal evolution of the Euclidean norm of the position error between these two methods are observed in Fig. 6: the ILC method (right) commanded more aggressive position corrections, yet fourteen iterations were necessary for robot task completion.

On the contrary, the IRLC solution proposed (left) provided a smoother convergence for all iterations that allowed a faster robot task completion (since its second iteration). Furthermore, Fig. 7 shows a comparison of the absolute input force, Eq. (8), difference $||\Delta F||$ between the proposed method and the alternative ILC at their respective final iteration, *i.e.*, the iteration where the peg insertion task was completed (without the peg impacting the box containing the hole before its insertion) for each formulation. It can be observed in Fig. 7 that the aggressive corrections performed by the alternative ILC method translated into much larger impedance force variation requirements (21.2 N on average) compared to the IRLC proposal (4.4 N on average).
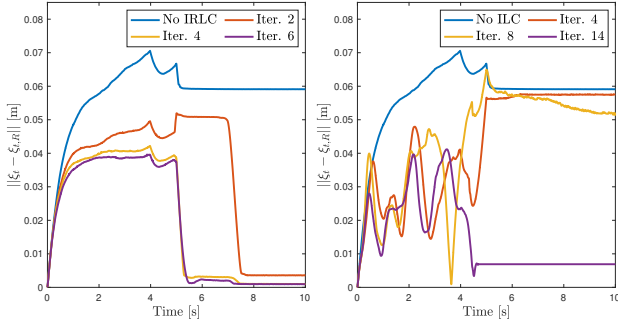

Fig. 6. Temporal evolution of the Euclidean norm of the position error of the robot end-effector, ξ_t, for a peg-in-hole task. Comparison between the proposed IRLC solution (left) and an ILC alternative (right).
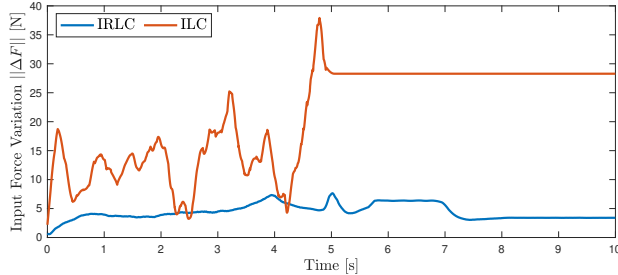

Fig. 7. Comparison of the input force difference $||\Delta F||$ between the proposed IRLC solution (blue) and an ILC alternative (red).

2) Choosing Different Cartesian Impedance Parameters: The impedance requirements of a robot task might change over time, which would imply the selection of a different set of robot impedance parameters, *i.e.*, its virtual stiffness K and damping D. As a result, the trajectory tracking behavior of the robot would be modified in this scenario, thus leading to the possibility that a, previously-successful, robot task might not be completed when the robot impedance parameters values are updated.

In this experiment, the translational Cartesian impedance parameters of the previous experiment were changed from 150 to 200 [N/m] for the virtual stiffness K, and from 50 to 70 [Ns/m] for the virtual damping D. The rotational impedance parameters were not modified from the previous experiment. Also, the initial Cartesian reference for this

experiment was chosen as the one used at the last iteration (*i.e.*, Iteration 6) of the previous experiment.

Figure 8 shows the temporal evolution of the position of the robot end-effector when varying the Cartesian impedance values in this peg-in-hole task, zoomed at the proximity of the inserted-peg position, see Fig. 4 (right). It is observed in Fig. 8 how the trajectory-tracking difference that occurred when selecting different robot impedance parameters caused the robot to not complete its task (*Iter. 0*). However, using the iterative reference learning strategy proposed in Sec. III, peg-in-hole task completion was achieved after only three additional iterations.
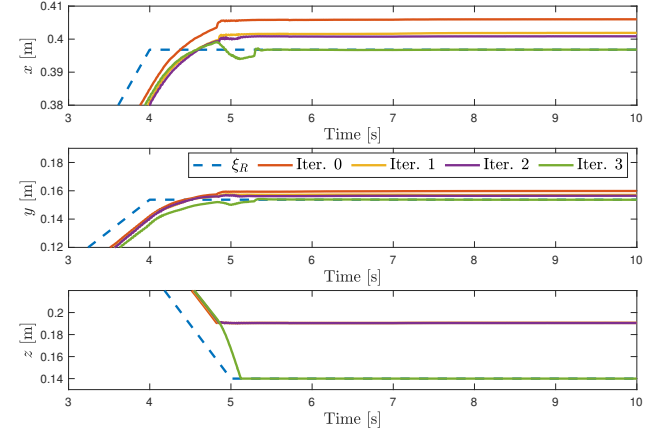

Fig. 8. Temporal evolution of the position of the robot end-effector along each Cartesian direction x, y, z with respect to its desired values for a peg-in-hole task with different Cartesian impedance values (zoom at the proximity of peg insertion).

C. Snap-Fit Assembly of a Switch

The use of the IRLC strategy proposed in Sec. III to improve robot trajectory tracking was also evaluated for the snap-fit assembly of a switch, where the same values for impedance (K and D) and learning parameters (β and R) as in the first experiments were selected. The workpieces involved in this assembly, which were components of an emergency stop button [31], can be seen in Fig. 9, *i.e.*, the switch, in a dark grey color and gripped by the robot, and a light gray piece with slots where the two lateral tabs of the switch should be inserted.

Fig. 9. Comparison between the final position of the switch before iterative learning was used (left) and after eight iterations of the proposed learning controller (right) for the snap-fit assembly of a switch.

Figure 10 shows the robot end-effector position throughout the switch snap-fit assembly experiments for different iterations. It can be seen in Fig. 10 that trajectory tracking improved at each iteration, which, as in the peg-in-hole experiment, is consistent with the monotonous decrease of the performance index ^{i}V of Eq. (21), and the negative performance index increment, $^{i}\Delta V$ of Eq. (26), shown in Fig. 11 for all learning iterations. Also, the robot was able to complete its task after only eight iterations.
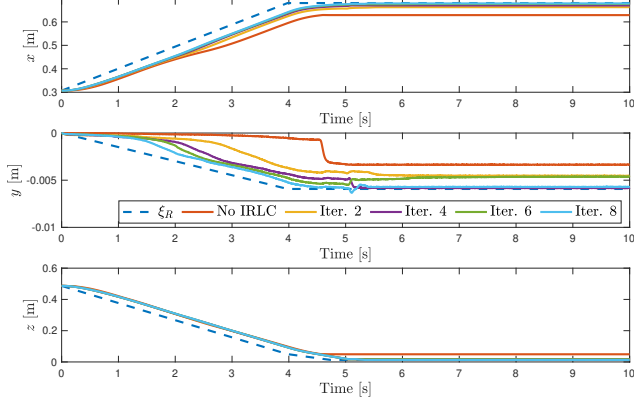

Fig. 10. Temporal evolution of the position of the robot end-effector along each Cartesian direction x, y, z with respect to its desired values for the snap-fit assembly of a switch.
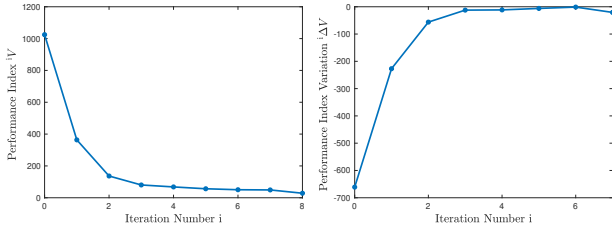

Fig. 11. Performance index (left), ^{i}V of Eq. (21), and performance index increment (right), $^{i}\Delta V$ of Eq. (26), for each iterative learning iteration i for the snap-fit assembly of a switch.

The trajectory-tracking requirements of this switch snap-fit assembly task were more demanding than in the previous peg-in-hole scenario in terms of the assembly tolerance and in the greater possibility of the two pieces involved in the robot task getting stuck, see, *e.g.*, Fig. 9 (left). As compared to the previously-presented peg-in-hole experiment, these assembly experiments would also require compensation for the external force needed to snap-fit the switch. For these reasons, a few more iterations (eight) than in the peg-in-hole scenario were needed to obtain an updated Cartesian reference that allowed robot task completion, even having already achieved accurate trajectory tracking in Iteration 4, as seen in Fig. 10.

V. DISCUSSION

In this paper, we have proposed an iterative learning strategy that modifies the Cartesian reference of a robot impedance controller to achieve robot task completion. The

proposed strategy has shown to improve the tracking of a robot Cartesian trajectory defined by human guidance in the context of kinesthetic teaching.

Moreover, the proposed strategy is compatible with a selection of robot impedance parameters (virtual stiffness K and damping D) that allowed a non-damaging interaction with the environment of the robot, which would have been a limitation of previously-proposed high-stiffness learning techniques [19]. A constant ratio between stiffness and damping parameters was chosen equal for all DOFs in [19]. Contrary to this, we introduced the matrix R in Eq. (15) to allow a different ratio for each DOF, being particularly significant since the problem in this paper was formulated in the Cartesian space instead of the joint space of the robot, as in [19]. Also, the introduction of Υ in Eq. (15) in our proposal contributed to relieving the high-stiffness requirements of the learning formulation in [19], thus allowing reference learning for kinesthetic teaching robot applications. Additionally, contrary to adaptive learning techniques [17], [18], our proposed selection of impedance parameters did not require any real-time modification.

Furthermore, the extensive evaluation experiments performed with a real collaborative robot manipulator showed that our proposal was able to achieve task completion for several robot tasks in a few iterations, which contrasted with the high number of iterations often required in other learning techniques, such as in Reinforcement Learning [11]. Additionally, as seen in the experimental comparison performed between the proposed method and an alternative ILC method [12], the linearity assumptions in the alternative ILC method [14], [15] allowed convergence guarantees for aggressive compensations that turned inferior in the experimental task performed, resulting in slower robot task completion and larger impedance force variation. In comparison, our proposal considered the nonlinearities of robot dynamics in its convergence analysis, which translated into a more conservative trajectory reference update that lead to faster (*i.e.*, in less iterations) convergence in robot task completion.

Additionally, it should be noted that the convergence conditions (18)–(20) of Theorem III.1 bounded the learning parameters (β and R) in our proposal. However, these learning parameters might be modified according to the robot task requirements. Therefore, future work aims at incorporating the impedance-controlled robot dynamics in the selection of the learning parameters to further improve iterative learning for bettering robot tracking of human manual demonstrations.

VI. CONCLUSION

Iterative learning can improve trajectory tracking for robot applications where impedance control is used by providing a Cartesian reference update. The proposed IRLC strategy was evaluated in several experiments using a real collaborative robot. These experiments showed a smooth convergence toward robot task completion in a small number of learning iterations, also compared to an alternative ILC method,

which highlighted the suitability of the proposed method for collaborative human–robot applications.

REFERENCES

[1] C. Schou, J. Damgaard, S. Bøgh, and O. Madsen, "Human-robot interface for instructing industrial tasks using kinesthetic teaching," in *44th IEEE Int. Symp. Robotics (ISR)*, Seoul, Korea, Oct. 19–27, 2013, pp. 1–6.

[2] B. D. Argall, S. Chernova, M. Veloso, and B. Browning, "A survey of robot learning from demonstration," *Robotics and Autonomous Systems*, vol. 57, no. 5, pp. 469–483, 2009.

[3] A. Cencen, J. C. Verlinden, and J. Geraedts, "Design methodology to improve human-robot coproduction in small-and-medium-sized enterprises," *IEEE/ASME Trans. Mechatronics (T-MECH)*, vol. 23, no. 3, pp. 1092–1102, 2018.

[4] N. Hogan, "Impedance control: An approach to manipulation: Parts I–III," *J. Dynamic Systems, Measurement, and Control*, vol. 107, no. 1, pp. 1–24, 1985.

[5] R. Johansson and M. W. Spong, "Quadratic optimization of impedance control," in *IEEE Int. Conf. Robotics and Automation (ICRA)*, San Diego, USA, Mar. 8–13, 1994, pp. 616–621.

[6] L. Villani and J. De Schutter, "Force control," in *Springer Handbook of Robotics*, B. Siciliano and O. Khatib, Eds. Berlin: Springer, 2016, ch. 9, pp. 195–217.

[7] S. Kawamura, F. Miyazaki, and S. Arimoto, "Is a local linear PD feedback control law effective for trajectory tracking of robot motion?" in *IEEE Int. Conf. Robotics and Automation (ICRA)*, Philadelphia, PA, USA, Apr. 24–29, 1988, pp. 1335–1340.

[8] O. Dahl, "Path constrained robot control," Doctoral Thesis, TFRT-1038, Dept. of Automatic Control, Lund University, 1992.

[9] A. Dahlin and Y. Karayiannidis, "Temporal coupling of dynamical movement primitives for constrained velocities and accelerations," *IEEE Robotics and Automation Letters (RA-L)*, vol. 6, no. 2, pp. 2233–2239, 2021.

[10] J. Ibarz, J. Tan, C. Finn, M. Kalakrishnan, P. Pastor, and S. Levine, "How to train your robot with deep reinforcement learning: lessons we have learned," *Int. J. Robotics Research*, vol. 40, no. 4-5, pp. 698–721, 2021.

[11] M. Pierallini, F. Angelini, R. Mengacci, A. Palleschi, A. Bicchi, and M. Garabini, "Iterative learning control for compliant underactuated arms," *IEEE Trans. Systems, Man, and Cybernetics: Systems (T-SMCA)*, 2023.

[12] S. Arimoto, S. Kawamura, and F. Miyazaki, "Bettering operation of robots by learning," *J. Robotic systems*, vol. 1, no. 2, pp. 123–140, 1984.

[13] D. A. Bristow, M. Tharayil, and A. G. Alleyne, "A survey of iterative learning control," *IEEE Control Systems Mag.*, vol. 26, no. 3, pp. 96–114, 2006.

[14] M. Norrlöf and S. Gunnarsson, "Disturbance aspects of iterative learning control," *Engineering Applications of Artificial Intelligence*, vol. 14, no. 1, pp. 87–94, 2001.

[15] P. Cano Marchal, O. Sörnmo, B. Olofsson, A. Robertsson, J. Gómez Ortega, and R. Johansson, "Iterative learning control for machining with industrial robots," *IFAC Proceedings Volumes*, vol. 47, no. 3, pp. 9327–9333, 2014.

[16] O. Sörnmo, A. Robertsson, and R. Johansson, "Increasing time-efficiency and accuracy of robotic machining processes using model-based adaptive force control," *IFAC Proceedings Volumes*, vol. 45, no. 22, pp. 543–548, 2012.

[17] B. Park, T.-Y. Kuc, and J. S. Lee, "Adaptive learning control of uncertain robotic systems," *Int. J. Control*, vol. 65, no. 5, pp. 725–744, 1996.

[18] R. Lee, L. Sun, Z. Wang, and M. Tomizuka, "Adaptive iterative learning control of robot manipulators for friction compensation," *IFAC-PapersOnLine*, vol. 52, no. 15, pp. 175–180, 2019.

[19] T.-Y. Kuc, K. Nam, and J. S. Lee, "An iterative learning control of robot manipulators," *IEEE Trans. Robotics and Automation (T-RO)*, vol. 7, no. 6, p. 835, 1991.

[20] C. Della Santina, M. Bianchi, G. Grioli, F. Angelini, M. Catalano, M. Garabini, and A. Bicchi, "Controlling soft robots: balancing feedback and feedforward elements," *IEEE Robot. Autom. Mag.*, vol. 24, no. 3, pp. 75–83, 2017.

[21] C.-C. Cheah and D. Wang, "Learning impedance control for robotic manipulators," *IEEE Trans. Robotics and Automation (T-RO)*, vol. 14, no. 3, pp. 452–465, 1998.

[22] S. Arimoto, P. Nguyen, and T. Naniwa, "Learning of robot tasks via impedance matching," in *IEEE Int. Conf. Robotics and Automation (ICRA)*, vol. 4. Detroit, MI, USA: IEEE, May 10–15, 1999, pp. 2786–2792.

[23] B. Siciliano and O. Khatib, *Springer Handbook of Robotics*. Springer, Berlin, 2016.

[24] O. Khatib, "A unified approach for motion and force control of robot manipulators: The operational space formulation," *IEEE J. Robotics and Automation*, vol. 3, no. 1, pp. 43–53, 1987.

[25] K. M. Lynch and F. C. Park, *Modern Robotics*. Cambridge University Press, Cambridge, UK, 2017.

[26] J. M. Salt-Ducaju, B. Olofsson, A. Robertsson, and R. Johansson, "Robot Cartesian compliance variation for safe kinesthetic teaching using Safety Control Barrier Functions," in *IEEE Int. Conf. Automation Science and Engineering (CASE)*, Mexico City, Mexico, Aug. 20–24, 2022, pp. 2259–2266.

[27] S. Wrede, C. Emmerich, R. Grünberg, A. Nordmann, A. Swadzba, and J. Steil, "A user study on kinesthetic teaching of redundant robots in task and configuration space," *J. Human-Robot Interaction*, vol. 2, no. 1, pp. 56–81, 2013.

[28] *Panda – Data Sheet*, Franka Emika, 2019.

[29] Y.-H. Lee, S.-C. Hsu, T.-Y. Chi, Y.-Y. Du, J.-S. Hu, and T.-C. Tsao, "Industrial robot accurate trajectory generation by nested loop iterative learning control," *Mechatronics*, vol. 74, p. 102487, 2021.

[30] T.-Q. Ta and S.-L. Chen, "Iterative learning control for integrated system of robot and machine tool," *Asian Journal of Control*, vol. 25, no. 2, pp. 807–823, 2023.

[31] A. Stolt, M. Linderoth, A. Robertsson, and R. Johansson, "Force controlled assembly of emergency stop button," in *IEEE Int. Conf. Robotics and Automation (ICRA)*, Shanghai, China, May 9–13, 2011, pp. 3751–3756.